JOURNAL OF MATERIALS SCIENCE 29 (1994) 4824–4833

Densification and mechanical properties of shock-treated alumina and its composites

M. BENGISU, O. T. INAL
New Mexico Institute of Mining and Technology, Materials and Metallurgical Engineering Department, Socorro, NM 87801, USA

The effects of shock treatment and consolidation method on densification behaviour and mechanical properties of Al_2O_3, Al_2O_3–ZrO_2, Al_2O_3–SiC (whisker), and Al_2O_3–ZrO_2–SiC (whisker) have been studied. It was established that shock treatment does not improve the sintering kinetics of alumina or alumina-based composites. On the other hand, partial shock compaction followed by sintering provided higher densities compared to sintering alone. Unshocked and pressureless sintered materials possessed better mechanical properties than shock-treated materials, in general. No significant difference was noted in the mechanical properties of hot-pressed Al_2O_3–ZrO_2 composites with regard to shock treatment. Improved mechanical properties were occasionally found in shock-treated and hot-pressed whisker-reinforced alumina, although a direct relationship with shock pressure was not observed. The improvement was attributed to decreased whisker aspect ratios upon shock treatment, leading to enhanced microstructural uniformity.

1. Introduction

Alumina-based composites are conventionally consolidated by pressureless sintering [1, 2] or hot pressing [3, 4]. The achievement of desired mechanical properties is strongly related to the relative density of the composites. Microstructural features such as grain size [5] and second-phase distribution [6], size [7, 8], and shape [9], are also important factors to consider. Toughness values as high as 9 and 14 MPa $m^{1/2}$ have been reported in whisker-toughened alumina (WTA) [5] and zirconia-toughened alumina (ZTA) [10], respectively. Composites with such high toughness, however, can only be produced with careful preconsolidation processing under suitable densification conditions.

Novel fabrication techniques such as hot isostatic pressing [11] (HIP), infiltration [12], rapid-rate sintering [13, 14], and microwave sintering [15] have been attempted to eliminate some of the disadvantages of conventional consolidation methods, e.g. remnant porosity in the case of pressureless sintering and shape restrictions, as well as high production costs in the case of hot pressing. Some studies also reported increased sintering rates of ceramic powders that were subjected to shock treatment [16, 17].

Although some studies analysing the effect of shock treatment on the densification of single-phase ceramics appear in the literature [16, 17], resultant mechanical properties are usually not available. Studies on the effect of shock treatment on the properties of composite ceramics are also unavailable. Thus, in order to investigate such aspects of shock treatment, the present study was undertaken.

2. Experimental procedure

2.1. Preconsolidation processing

Al_2O_3 powders (RC-HP-DBM, Malakoff Ind., West Malakoff, TX) were mixed with ZrO_2 powders (SC15, Magnesium Elektron, Inc., Flemington, NJ) and/or SiC whiskers (SCW 10 and SCW 1-0.6, Tateho Chemical Ind., Co., Ltd, Japan) to yield Al_2O_3–5, 10, and 15 vol % ZrO_2, Al_2O_3–10, 20, and 30 vol % SiC_w, and Al_2O_3–10/15 vol % ZrO_2–10, 20 vol % SiC_w composites. Slurries were prepared using methanol in a high-speed blender. Methanol was selected as the dispersing medium because it was shown to be suitable for oxide systems [18]. After reaching a suitable slurry viscosity, by adjusting the liquid content, spray drying was conducted to achieve a fine mixture of composite powders. A uniform powder or even a powder/whisker mixture is achieved by this process, which is an important step in composite fabrication for the achievement of desired properties.

2.2. Shock treatment

Powders were uniaxially pressed into 5 cm diameter and 0.6 cm thick mild steel containers under a pressure of 40 MPa to achieve approximately 50% theoretical density (TD). The inner parts of the containers were lined with graphite foil to yield two pieces, about 1 cm thick, in each composition, in order to make the fabrication of partially shock-compacted pellets possible. Axisymmetric loading was employed with ANFO explosive. Each composition was shock treated under calculated pressures [19] of 4, 7, and 10 GPa.

0022–2461

After shock conditioning, containers were sectioned with SiC abrasive wheels at high speed. On several occasions, the cutting action caused fracture inside the compacts; some samples, however, could be recovered without fracture. The remaining pieces were fragmented, milled, and sieved through a 100 mesh sieve.

2.3. Post-shock consolidation

Pellets were prepared from unshocked and shock-treated powders by uniaxial pressing at 20 MPa. Two samples from each composition and shock pressure were sintered in a graphite-element furnace under flowing argon.

All whisker-containing compositions were consolidated by hot pressing. Additionally, A-10Z samples were hot pressed for comparison with pressureless consolidation methods. A-10Z samples were hot pressed at 1500 °C, while whisker-containing samples were hot pressed at 1800 °C. All hot pressing was performed with graphite dies and rams, at a pressure of 30 MPa in flowing argon gas. Heating times were about 60 min and hold times were 30 min.

2.4. Shock compaction and subsequent sintering

Pellets 10 mm thick with 50 mm diameter were carefully extracted from steel containers after shock treatment. Some of these contained spiral cracks imparted by non-uniform shock waves. Some of them were recovered with no visible cracks. Partial densification was achieved in these pellets. Whisker–containing compacts were subjected to pressureless sintering at 1800 °C for 30 min in flowing argon, embedded in alumina powder within a graphite container, to reduce possible reaction with the crucible and carbon-rich furnace gases. A graphite heating-element furnace was used to sinter these samples. Pressureless sintering of partially shock compacted alumina and ZTA pellets, and some whisker-containing composites was performed at 1600 °C for 30 min in air.

2.5. Characterization

Densities of consolidated samples were measured using Archimedes' principle [20]. Fracture surfaces were analysed by SEM (Model HHS-2R, Hitachi, Ltd., Tokyo, Japan). Some WTA specimens were etched by boiling in diluted phosphoric acid for 5 min to reveal the whiskers. Phase analysis was performed by X-ray diffractometry (Model PW1410180, Philips, Inc., Waltham, MA). The amount of tetragonal ZrO_2 (t-ZrO_2) in ZrO_2-containing composites were calculated from relative intensities of monoclinic ZrO_2 (m-ZrO_2) and t-ZrO_2 peaks [21].

Microhardness values were determined by a Vickers micro-indentor on polished surfaces, under a load of 1 kg for 10 s. The indentation-strength-in-bending (ISB) method [22, 23] was used for fracture toughness evaluation of air-sintered and hot-pressed specimens. Three measurements per composition and shock pressure were made. Bars 3 mm × 3 mm × 20 mm in dimension were indented on one of their surfaces under 100 N loads to ensure well-developed cracks and loaded with a three-point bend apparatus. Three-point bend testing of polished bars was conducted to determine flexural strength. At least two samples per composition and shock pressure were used for strength measurements. Loading of whisker-containing samples was conducted at a direction perpendicular to the whisker orientation (caused due to hot pressing) for fracture toughness and strength evaluation.

3. Results and discussion

3.1. Densification results

Table I lists densities achieved in shock-treated and unshocked powder compacts upon sintering. As the results indicate, shock compaction as well as the addition of ZrO_2 decreases the sinterability of Al_2O_3. For example, unshocked A-5Z densified up to 98.5% theoretical density (TD), whereas 10 GPa shock-treated A-5Z could only be sintered up to 87.2% TD. Furthermore, the sintered density of unshocked Al_2O_3 decreased from close to full TD to 98% TD upon 15 vol % ZrO_2 additions. The simultaneous effect of shock treatment and ZrO_2 addition is evident in samples shock-treated at higher pressures (7 and 10 GPa). The content of ZrO_2 does not seem to change the degree of reduced sintering by high-pressure shock treatment. Nevertheless, the presence of ZrO_2 (5 vol % or over in this study) in Al_2O_3 magnifies the deleterious effect of shock treatment.

Lange [24] showed that crack-like internal defects were present at fracture origins in sintered ZTA composites, and attributed these defects to differential

TABLE I Fractional density of Al_2O_3 and Al_2O_3–ZrO_2 composites

Material	Densification method	Shock pressure (GPa)	ρ_{th} (%)[a]
Al_2O_3	Air sintering	0	100 ± 0.0
	60 min/1600 °C	4	99.7 ± 0.2
		7	98.0 ± 0.4
		10	100 ± 0.0
A-5Z	Air sintering	0	98.5 ± 0.5
	60 min/1600 °C	4	96.3 ± 3.3
		7	96.9 ± 0.2
		10	87.2 ± 0.8
A-10Z	Air sintering	0	97.0 ± 1.0
	60 min/1600 °C	4	93.8 ± 5.0
		7	84.7 ± 5.6
		10	88.4 ± 0.3
	Hot pressing	0	99.2[b]
	30 min/1500 °C	4	99.2[b]
		7	99.6[b]
		10	99.5[b]
A-15Z	Air sintering	0	98.0 ± 0.1
	60 min/1600 °C	4	95.7 ± 1.6
		7	89.6 ± 0.6
		10	88.4 ± 1.1

[a] Average values from two samples.
[b] Data from one sample.

sintering of agglomerates. Similarly, ZrO_2 agglomerates were observed to shrink away in Al_2O_3 matrices during sintering [25], decreasing sinterability. The presence of shock-induced hard agglomerates can have a similar effect on sintering. Because partial compaction occurs during shock treatment, powders obtained by grinding and sieving of shock-treated ceramics still contain some of these agglomerates. In the present case, the agglomerate size is $\leqslant 74\ \mu m$, determined by the sieve openings. These agglomerates persist to the final stages of sintering. While Al_2O_3–5 vol % ZrO_2 (A-5Z) samples shocked at 4 GPa are not significantly altered by the shock treatment (Fig. 1a), agglomeration is evident in those shocked at 7 and 10 GPa (Fig. 1b and c). Agglomerated regions differ from the matrix by grain growth at the interior (Fig. 2) owing to faster densification compared to the matrix. While the matrix porosity continues to decrease, agglomerates fully densify at one point during sintering, after which grain coarsening occurs. An earlier study [26] has shown that such agglomerates, whether introduced by shock treatment or other procedures such as sintering followed by crushing, milling, and sieving, are deleterious to the sintering of pure Al_2O_3.

Hot pressing of shock treated and unshocked A-10Z, A-10S (Al_2O_3–10 vol % SiC_w), A-20S, and A-30S composites yielded quite different results compared to pressureless sintering. Table II shows that the simultaneous application of pressure and high temperature neutralizes the effect of agglomerates. Although no shock-activated sintering can be detected, deleterious effects are not observed either. The influence of pressure during sintering can be understood from its direct contribution to the driving force for densification, i.e. increasing the contact stress between particles [27]. Another important effect is the rearrangement of particles and reduction of large interagglomerate pores. Partial closure of pores will reduce the pore coordination number so that they can spontaneously disappear during sintering [28]. Therefore, the adverse effect of agglomerates can be eliminated by hot pressing. In the case of whisker-containing composites, a higher resistance to densification exists due to the skeletal network formed by the whiskers. The present experimental results reveal that as the amount of whiskers is increased, the resistance becomes more pronounced even when hot pressing is employed. Table II shows that while the average fractional density of A-10S composites is 98.7%, it decreases to 97.8% (about 1%) in A-30S composites.

Direct sintering of as shock-compacted pellets was also studied as a densification process. While in many cases shock-compacted samples contained cracks, some samples were recovered without visible cracks. However, SEM analysis showed internal cracks in such samples. Shock-compacted pellets were sintered to improve their densities. Table III shows that high levels of relative densities can be achieved by this process. In the case of ZTA, higher densities were achieved compared to air-sintered samples. This may be attributed to the high initial densities of shock-compacted samples (70%–80% TD for shock-compacted, compared to 50% TD for uniaxially pressed pellets). While WTA composites could not be sintered to high densities, an Al_2O_3–15 vol % ZrO_2–20 vol % SiC_w (A-15Z-20S) composite was sintered to over 96% TD at 1800 °C in 30 min. Although useful densities can be achieved by this process, formation of cracks is very difficult to prevent during shock-compaction of brittle materials.

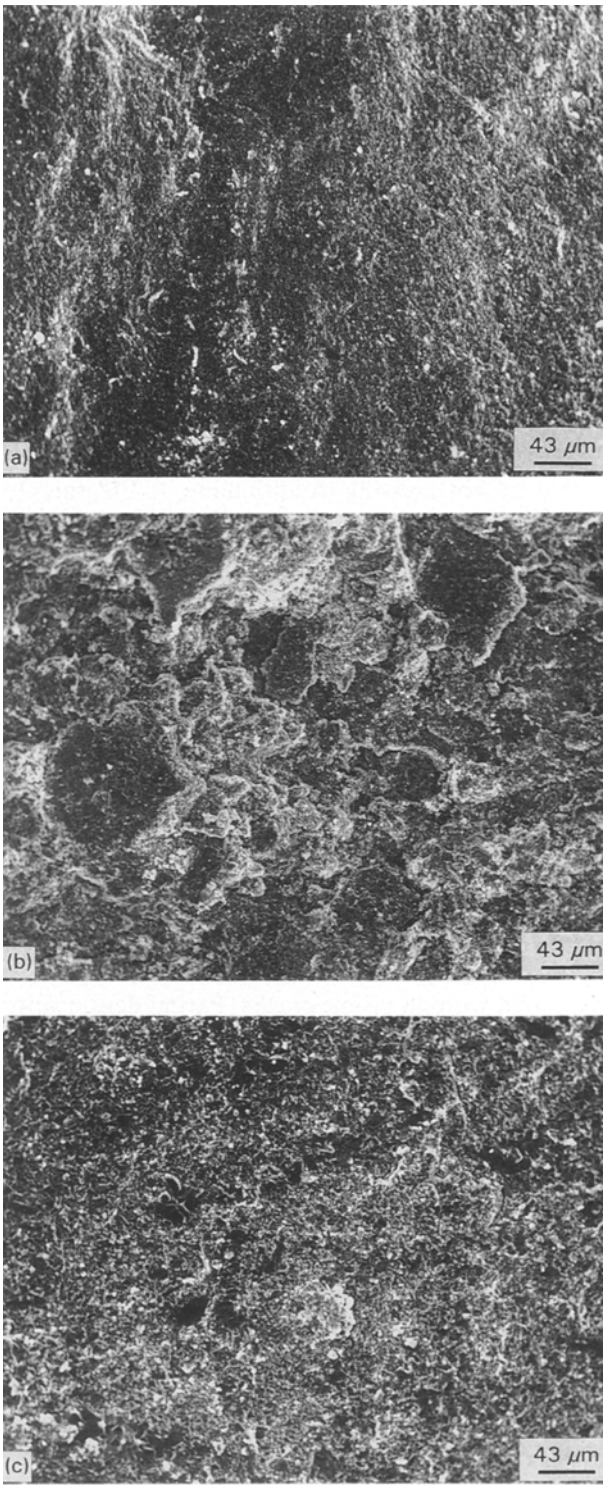

Figure 1 Scanning electron micrograph of the fracture surface of (a) 4 GPa shock-treated and air-sintered Al_2O_3–5 vol % ZrO_2 composite showing uniform microstructure with little or no indication of agglomeration, (b) 7 GPa, and (c) 10 GPa shock-treated and air-sintered Al_2O_3–5 vol % ZrO_2 composites showing large agglomerates due to local densification.

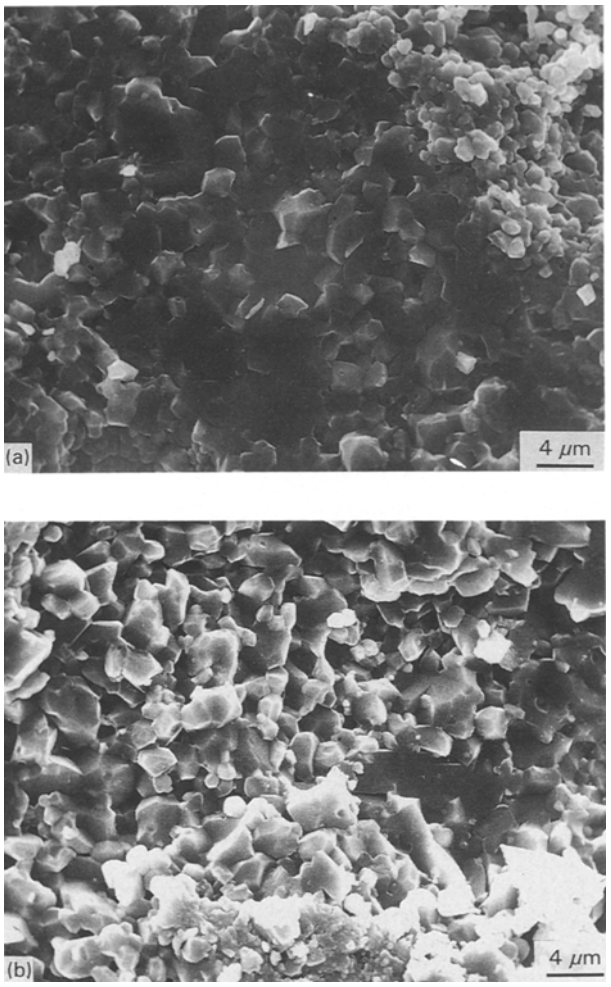

Figure 2 Scanning electron micrographs of (a) 7 GPa and (b) 10 GPa shock-treated and air-sintered Al_2O_3–5 vol % ZrO_2 composites exhibiting local grain growth at the interior of agglomerates shown in Fig. 1.

TABLE II Fractional density of Al_2O_3–SiC_w and Al_2O_3–ZrO_2–SiC_w composites[a]

Material	Shock pressure (GPa)	ρ_{th} (%)
A-10S	0	98.3
	4	98.9
	7	99.2
	10	98.5
A-20S	0	99.3
	4	99.1
	7	98.7
	10	98.9
A-30S	0	98.8
	4	97.2
	7	97.9
	10	97.2
A-10Z-20S	0	97.9
	4	97.9
	7	N/A[b]
	10	N/A
A-10Z-10S	0	N/A
A-15Z-20S	0	N/A
A-15Z-10S	0	N/A

[a] All samples hot pressed at 1800 °C for 30 min, density data from one sample per composition and shock pressure.
[b] Exact composition unknown owing to new phases formed during hot pressing.

TABLE III Fractional density of shock compacted and subsequently sintered samples

Material	Sintering temperature (°C)/time (min)/atmosphere	Shock pressure (GPa)	ρ_{th} (%)
Al_2O_3	1600/30/air	4	99.1
		7	96.2
		10	95.7
A5Z	1600/30/air	4	99.6
		7	99.5
		10	96.5
A10Z	1600/30/air	4	99.1
		7	98.9
		10	98.8
A15Z	1600/30/air	4	96.3
		7	99.3
		10	96.0
A10Z10S	1600/30/air	4	73.6
		7	88.8
		10	87.9
A10Z20S	1600/30/air	4	73.0
		7	83.1
		10	88.1
A15Z10S	1600/30/air	4	84.2
		7	87.7
		10	88.3
A15Z20S	1600/30/air	4	75.1
		7	82.0
		10	88.7
	1800/30/Ar	10	95.7
A10S	1800/30/Ar	4	62.0
		7	68.7
		10	78.4
A20S	1800/30/Ar	4	60.7
		7	70.3
		10	85.2
A30S	1800/30/Ar	4	53.3
		7	71.5
		10	83.0

3.2. Microstructure

X-ray analysis of air-sintered ZTAs indicated that the fraction of t-ZrO_2 to m-ZrO_2 decreased as the amount of ZrO_2 in Al_2O_3 increased. This may be due to the lower relative densities attained in shock-treated and unshocked ZTA composites with increasing ZrO_2 content, resulting in a reduced matrix constraint on ZrO_2 particles. It was also observed that shock treatment did not increase the amount of retained t-ZrO_2. This result is different from that achieved in shock-compacted and subsequently sintered samples where increased t-ZrO_2 retention was observed with increasing shock pressures [29]. The difference is due to an additional milling operation in the present case, transforming any retained t-ZrO_2 to m-ZrO_2 under stress.

SEM analysis of WTA composites revealed that shock treatment resulted in a lowering of whisker aspect ratios (Fig. 3). Better homogeneity was achieved by the use of shock-processed, low aspect ratio whiskers in alumina.

Some surprising results were found from X-ray analysis of ZrO_2-and-whisker-toughened alumina

TABLE IV X-ray diffraction analysis results for alumina-based composites

Material	Fabrication method	Shock pressure (GPa)	Weight reduction (%)	Major peaks, d (nm)	Observed relative intensity (%)	Fitting peaks	d (nm)	Relative intensity (%)
A10Z20S	Hot pressing/ 1800 °C/30 MPa 30 min/Ar	0	9.4	0.209	100.0	α-Al_2O_3 (1 1 3)	0.209	100
				0.315	15.6	m-ZrO_2 ($\bar{1}$ 1 1)	0.316	100
				0.295	10.2	t-ZrO_2 (1 0 1)	0.299	100
				0.270	11.8	(ZrC) 8F	0.271	100
				0.251	30.7	α-SiC (1 0 0)	0.253	100
		4	9.8	0.209	100.0	α-Al_2O_3 (1 1 3)	0.209	
				0.316	17.1	m-ZrO_2 ($\bar{1}$ 1 1)	0.316	
				0.295	10.8	t-ZrO_2 (1 0 1)	0.299	
				0.270	11.6	(ZrC) 8F	0.271	
				0.251	31.1	α-SiC (1 0 0)	0.253	
		7	48.7	0.209	100.0	α-Al_2O_3 (1 1 3)	0.209	
				0.316	5.9	m-ZrO_2 ($\bar{1}$ 1 1)	0.316	
				0.270	23.2	(ZrC) 8F	0.271	
				0.252	72.5	α-SiC (1 0 0)	0.253	
		10	46.4	0.209	100.0	α-Al_2O_3 (1 1 3)	0.209	
				0.315	6.4	m-ZrO_2 ($\bar{1}$ 1 1)	0.316	
				0.270	16.5	(ZrC) 8F	0.271	
				0.252	57.2	α-SiC (1 0 0)	0.253	
A10Z10S	Hot pressing	0	36.8	0.209	100.0	α-Al_2O_3 (1 1 3)	0.209	100
				0.270	17.0	(ZrC) 8F	0.271	100
				0.252	25.0	α-SiC (1 0 0)	0.253	100
A15Z10S	Hot pressing	0	61.0	0.209	100.0	α-Al_2O_3 (1 1 3)		
				0.271	48.0	(ZrC) 8F		
				0.235	55.0	(ZrC) 8F	0.235	80
				0.252	40.0	α-SiC (1 0 0)		
A15Z20S	Hot pressing	0	49.8	0.209	100.0	α-Al_2O_3 (1 1 3)		
				0.315	6.0	m-ZrO_2 ($\bar{1}$ 1 1)	0.316	100
				0.297	5.0	t-ZrO_2 (1 0 1)	0.299	100
				0.270	36.0	(ZrC) 8F		
				0.234	31.0	(ZrC) 8F		
				0.251	55.0	α-SiC (1 0 0)		
A15Z10S	Hot pressing and air annealing	0		0.209	100.0	α-Al_2O_3 (1 1 3)		
				0.319	14.0	m-ZrO_2 ($\bar{1}$ 1 1)		
				0.297	9.0	t-ZrO_2 (1 0 1)		
				0.253	41.0	α-SiC (1 0 0)		
A10Z10S	Shock compaction and air sintering, exterior (white)	10		0.209	74.8	α-Al_2O_3 (1 1 3)	0.209	100
				0.317	32.3	m-ZrO_2 ($\bar{1}$ 1 1)	0.316	100
				0.298	52.3	t-ZrO_2 (1 0 1)	0.299	100
				0.271	34.0	(ZrC) 8F	0.271	100
				0.235	16.9	(ZrC) 8F	0.235	80
				0.344	53.0	Mullite (1 2 0)	0.343	100
A10Z10S	Shock compaction and air sintering, interior (green)	10		0.209	87.1	α-Al_2O_3 (1 1 3)		
				0.316	28.2	m-ZrO_2 ($\bar{1}$ 1 1)		
				0.297	23.5	t-ZrO_2 (1 0 1)		
				0.239	36.1	α-SiC (1 0 0)		
A15Z20S	Shock compaction and sintering in graphite-element furance/flowing Ar shell (black)	10		0.209	76.9	α-Al_2O_3 (1 1 3)		
				0.317	23.3	m-ZrO_2 ($\bar{1}$ 1 1)		
				0.297	13.3	t-ZrO_2 (1 0 1)		
				0.270	59.4	(ZrC) 8F		
				0.234	67.0	(ZrC) 8F		
A15Z20S	Shock compaction and sintering in graphite-element furnace/flowing Ar interior (green)	10		0.209	89.3	α-Al_2O_3 (1 1 3)		
				0.316	34.8	m-ZrO_2 ($\bar{1}$ 1 1)		
				0.296	22.2	t-ZrO_2 (1 0 1)		
				0.270	18.3	(ZrC) 8F		
				0.235	24.1	(ZrC) 8F		

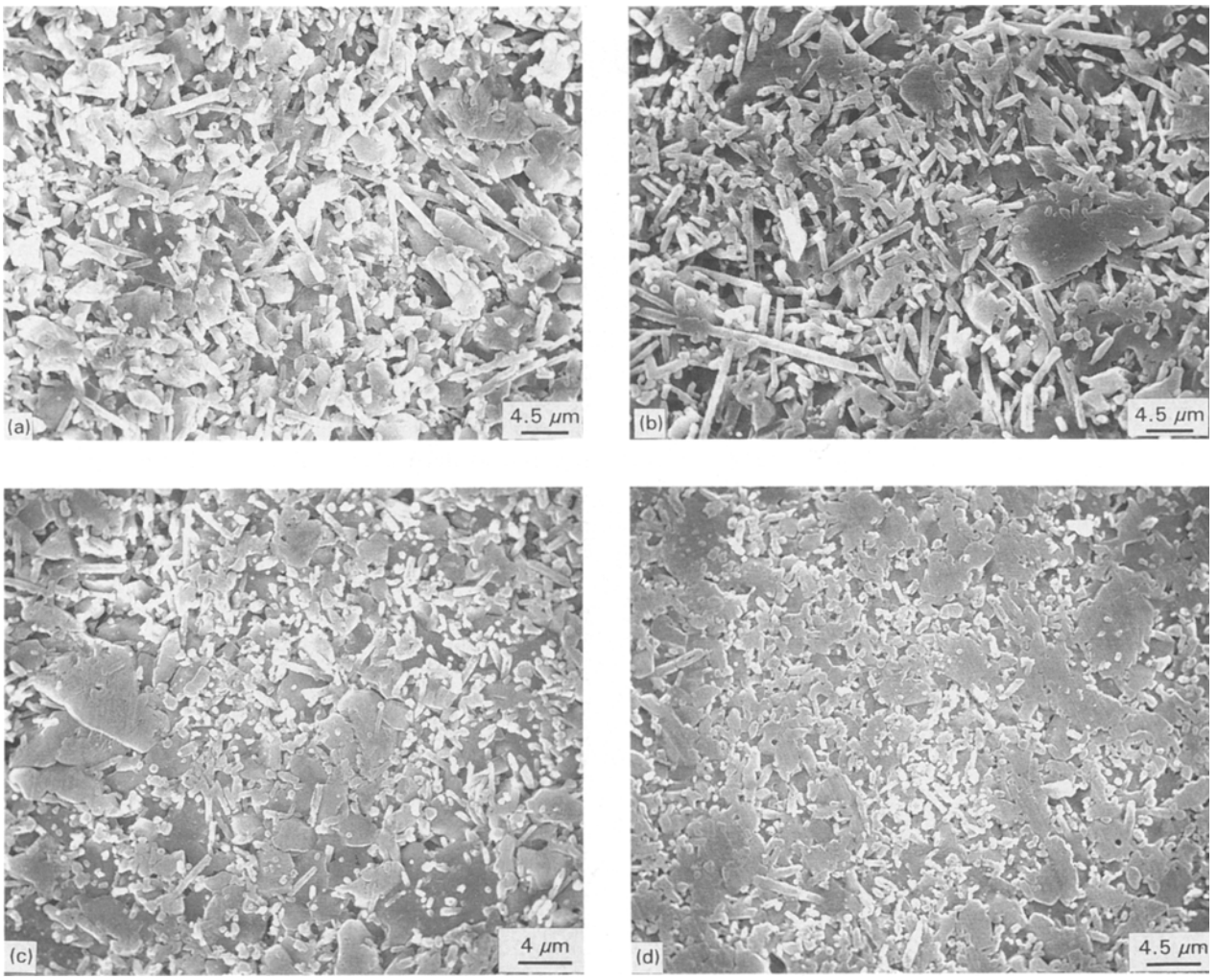

Figure 3 Effect of shock treatment on whisker aspect ratios in Al_2O_3–20 vol % SiC_w composites.

(ZWTA) composites. In these composites, ZrO_2 reacted with carbon, supplied either by the hot-pressing environment or by SiC, to form ZrC. In some cases, this was accompanied by extreme weight reduction and deformation of the samples. Table IV shows phase identification results for the composites and weight reduction accompanying hot pressing. The table indicates that all ZrO_2 was transformed to ZrC in A-10Z-10S and A-15Z-10S composites. While unshocked and 4 GPa shock-treated A-10Z-20S composites, which were hot pressed simultaneously, only lost 9.4% and 9.8% of their initial weight, 7 and 10 GPa shock-treated A-10Z-20S composites, also hot pressed simultaneously, lost 48.7% and 46.4% of their initial weight. The source of such a difference is unknown, but it may be due to the different conditions experienced during hot pressing, such as an unintentional increase in the partial pressures of carbon-rich furnace gases.

Hot-pressed ZTA composites did not reveal any evidence of ZrC formation, but their consolidation temperature was 1500 °C, rather than 1800 °C used for ZWTA and WTA composites. Partially shock-compacted and subsequently air-sintered ZWTA samples contained both mullite and ZrC in their white-coloured exterior (Table IV). No SiC was left in this region, probably due to the consumption of silicon atoms by mullite. In contrast, the interior of these samples did not contain any ZrC or mullite. Similar results were observed by Backhaus-Ricoult [30] in ZWTA that was annealed in air at 1400–1600 °C for 10–20 h. ZrC was again formed in partially shock-compacted and subsequently sintered samples, when sintering was conducted in a graphite-heating element furnace with flowing argon. It is not clear if ZrC formation during hot pressing occurs from the reaction of ZrO_2 with SiC, with carbon from graphite dies and rams, or with carbon-rich furnace gases. The latter two sources seem to be more plausible because X-ray results do not suggest a decrease or elimination in the SiC phase.

Annealing of a piece of A-15Z-10S composite at 800 °C for 2 h resulted in another surprising phenomenon. The composite decomposed entirely and only ash-like powder was recovered. X-ray analysis of the powder revealed that part of the ZrC (formed during hot pressing) re-reacted to form ZrO_2. The rest of the powder consisted of Al_2O_3 and SiC. This result shows that the formation of ZrC in ZWTA is detrimental to the composite, especially if the composite is designed for high-temperature use in oxidizing environments.

3.3. Mechanical properties

3.3.1. Flexural strength

3.3.1.1. ZTA Composites. Table V lists the strength values of ZTAs obtained from three-point bend tests. A striking feature seen in the table is that all the best strength values correspond to unshocked materials in the case of air-sintered samples. The average strength levels of shock-treated and air-sintered materials are about half of that of their unshocked counterparts. Because the grain sizes of shocked and unshocked samples are similar, shock-generated agglomerates and related porosity comprise the only apparent difference that can cause such a marked decrease in strength. The detrimental effect of agglomerates on the mechanical properties of ceramic materials has been well-documented [24, 31]. The lowest strength values belong to ZTAs with the highest porosity (Table V). However, shock treatment at 4 GPa, while not decreasing the fractional densities, markedly reduced strength values in all cases, indicating the drastic effect of agglomerates on strength. Strength data from hot-pressed A-10Z composites further support this implication; in this case, the strength values are very similar, suggesting that reduced local densification by pressure eliminates the adverse effect of shock-produced agglomerates.

Air-sintered ZTA composites with 30%–44% t-ZrO_2 (based on the total amount of ZrO_2) exhibited a peak strength of 530 MPa at 5 vol % ZrO_2 and a subsequent decrease with increasing ZrO_2 (Table V). This value is in agreement with literature data [32, 33]. Hot-pressed A-10Z composites exhibited improved strength values compared to air-sintered A-10Z, probably due to reduced porosity and a reduced number of agglomerates. The present results show that, while it is possible to strengthen alumina by the addition of zirconia, the presence of residual porosity and shock-induced agglomerates are detrimental to the strength.

3.3.1.2. WTA and ZWTA composites. Results of the present study show that a higher percentage of whiskers in alumina causes a decrease in flexural strength. Table VI shows that this trend is especially apparent in the case of unshocked composites. Strength results from shock-treated samples do not show such a clear pattern. The highest flexural strength values were found in 10 GPa shock-treated A-20S composites, suggesting that shock treatment improved the composite strength, although other composites did not yield similar results. All shock-treated WTA samples, however, exhibited higher strength than unshocked samples, as illustrated in Table VI. The improvement in strength may be linked to better homogeneity achieved due to lower whisker aspect ratios in shock-treated WTAs (Fig. 3).

The average values obtained from all samples (shocked and unshocked) yielded strength values of 444, 454, and 350 MPa for 10, 20, and 30 vol % SiC_w, respectively. The decreased strength values in A-30S composites can be attributed to increased whisker clustering, associated with a higher number of whiskers per unit volume.

Strength values of ZWTA composites are also shown in Table VI. A-10Z-20S composites shock-treated at 7 and 10 GPa have lower strength compared to unshocked and 4 GPa shock-treated composites. This is probably due to a large amount of ZrC formation in the former two composites. The lowest strength values among ZWTAs were found in A-10Z-10S, A-15Z-10S, and A-15Z-20S composites, in which most or all of the ZrO_2 reacted to form ZrC (Table IV).

TABLE V Mechanical properties of Al_2O_3 and Al_2O_3–ZrO_2 composites

Material	Densification method	Shock pressure (GPa)	t-ZrO_2 in total ZrO_2 (%)	ρ_{th} (%)	Flexural strength (MPa)	Upper/ lower limits	Fracture toughness (MPa $m^{1/2}$	Upper/ lower limits
Al_2O_3	Air sintering	0		100	431	524/351	5.1	5.4/4.7
	1600 °C/60 min	4		99.7	262	274/250	5.2	5.6/5.0
		7		98.0	243	306/206	4.3	4.8/3.7
		10		100	258	278/246	4.7	4.8/4.6
A5Z	Air sintering	0	44	98.5	530	N/A	5.3	6.1/4.8
		4	42	96.3	257	304/209	4.3	4.6/4.1
		7	43	96.9	292	N/A	5.2	5.3/5.1
		10	45	87.2	151	N/A	3.8	4.2/3.3
A10Z	Air sintering	0	43	97.0	443	458/429	5.5	5.6/5.4
		4	38	93.8	303	358/248	5.0	5.1/4.8
		7	44	84.7	117	200/51	4.3	4.5/3.8
		10	38	88.4	109	130/95	4.0	4.7/3.4
	Hot pressing	0	47	99.2	556	597/528	6.7	7.1/6.3
	1500 °C/30 MPa/	4	38	99.2	553	565/541	6.5	7.2/6.1
	30 min	7	30	99.6	368	490/211	7.2	7.7/6.7
		10	33	99.5	533	562/517	6.9	7.0/6.7
A15Z	Air sintering	0	19	98.0	273	311/251	6.1	6.9/5.5
		4	24	95.7	230	262/198	4.3	4.9/3.7
		7	19	89.6	78	116/40	3.9	4.0/3.8
		10	25	88.4	129	169/63	2.8	2.8/2.7

TABLE VI Mechanical properties of Al_2O_3–SiC_w and Al_2O_3–ZrO_2–SiC_w composites[a]

Material	Shock pressure (GPa)	Chemical Reaction yes/no	ρ_{th} (%)	Flexural strength (MPa)	Upper/ lower limits	Fracture toughness (MPa $m^{1/2}$)	Upper/ lower limits
A10S	0	No	98.3	434	473/407	6.1	6.4/6.0
	4		98.9	467	486/445	7.0	7.2/6.8
	7		99.2	435	478/399	5.6	5.9/5.3
	10		98.5	439	515/337	5.7	6.2/5.2
A20S	0	No	99.3	310	383/202	4.8	N/A
	4		99.1	463	511/405	5.0	5.4/4.4
	7		98.7	412	456/345	4.7	4.9/4.5
	10		98.9	631	725/558	5.0	5.6/4.6
A30S	0	No	98.8	197	321/105	4.5	5.1/4.2
	4		97.2	400	444/341	5.1	5.4/4.7
	7		97.9	467	496/415	5.5	6.0/4.6
	10		97.2	359	441/224	5.1	6.0/4.5
A10Z20S	0	Yes	97.9	472	508/445	5.6	6.3/5.1
	4		97.9	446	512/396	6.6	7.2/6.0
	7	Yes	N/A	413	479/352	6.3	6.6/5.7
	10		N/A	410	452/369	8.0	8.9/7.0
A10Z10S	0	Yes	N/A	259	305/213	5.8	6.9/5.0
A15Z20S	0	Yes	N/A	253	463/42	5.6	6.0/5.1
A15Z10S	0	Yes	N/A	363	381/345	6.2	7.4/5.2
A15Z20S[b]	10	Yes	95.7	N/A	N/A	5.1	5.8/4.7

[a] All samples hot pressed at 1800 °C/30 min, except indicated[b].
[b] Shock-compacted and sintered at 1800 °C for 30 min in Ar.

3.3.2. Fracture toughness

3.3.2.1. ZTA composites. As the amount of ZrO_2 in alumina increased in the air-sintered, unshocked samples, the toughness increased (Table V). The same was not true for shock-treated samples due to remnant porosity. Significantly lower fracture toughnesses were found in 10 GPa shock-treated samples, which had the highest porosity among air-sintered ZTAs. While pressureless-sintered A-10Z composites, with 2%–3% porosity yielded fracture toughness values of 5–5.5 MPa $m^{1/2}$, hot-pressed A-10Z with 0.4%–0.5% porosity had a toughness of 7 MPa $m^{1/2}$, indicating the importance of complete densification. Slightly improved fracture toughness values were obtained in 7 and 10 GPa shock-treated and hot-pressed A-10Z composites. This can be attributed to the 0.3%–0.4% increase in fractional densities which may be an indication of shock-activated consolidation. The fraction of t-ZrO_2/m-ZrO_2 in shock-treated A-10Z was not higher than that in unshocked A-10Z, eliminating the possibility of increased toughening due to an increased amount of t-ZrO_2. The reason for the occasional positive densification response of shock-treated samples in hot-pressed samples is the high pressure, preventing local densification and making better use of shock-induced defects during consolidation.

3.3.2.2. WTA and ZWTA composites. The best toughness values in WTA composites were achieved in A-10S (Table VI). Increased whisker contents decreased fracture toughness values, in analogy to strength values. The inferior mechanical properties of WTAs with higher volume fractions of whiskers can be attributed to increased whisker clustering. Fig. 4 shows the difference of fracture surfaces between A-10S and A-20S composites. It can be seen that very little evidence of whisker pull-out exists in the case of A-20S, while whisker debonding and pull-out are evident in A-10S composites. Comparison of indentation-crack paths in A-10S and A-20S shows similar evidence (Fig. 5); crack deflection, whisker pull-out, and crack bridging mechanisms, which can all contribute to toughness, are observed in A-10S composites, but none are seen in A-20S composites. This explains the difference in the mechanical properties of low (10 vol %) and high (20–30 vol %) whisker content WTAs. Slightly higher fracture toughness values were obtained in all 4 GPa shock-treated WTA samples when compared to unshocked samples. This, again, may be the result of reduced whisker aspect ratios, resulting in better microstructural uniformity.

High toughness values expected from additive or multiplicative toughening, due to the presence of both ZrO_2 and whiskers in alumina, were not achieved in ZWTAs (Table VI). All of these composites contained ZrC due to the reaction of ZrO_2 with carbon. Unshocked and 4 GPa shock-treated A-10Z-20S composites contained the least amount of ZrC and their weight loss was also the lowest in ZWTAs. The relatively low fracture toughness values in A-10Z-10S, A-15Z-10S, and A-15Z-20S can be attributed to the severe chemical reaction that caused extensive weight loss and deformation of the composites. The reason for lower-than-expected toughness levels in the composites with little ZrC, however, are speculated to be due to counteractive toughening mechanisms, which are discussed in detail elsewhere [34]. Such counter-

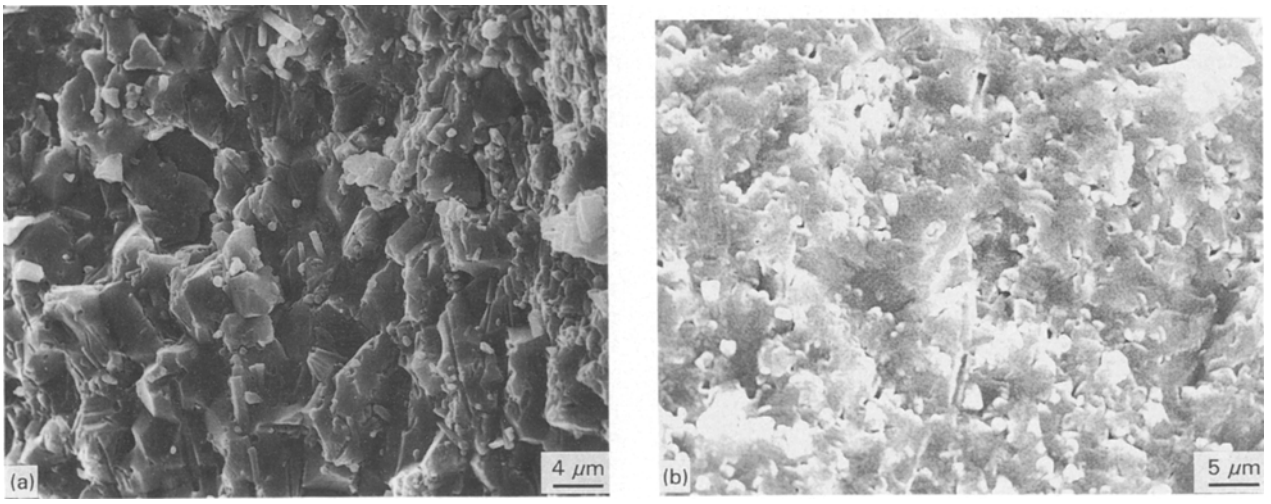

Figure 4 Scanning electron micrographs of fracture surfaces of hot-pressed (a) Al_2O_3–10 vol % SiC_w showing significant whisker pull-out and debonding phenomena, and (b) Al_2O_3–20 vol % SiC_w with very little evidence of debonding and no whisker pull-out.

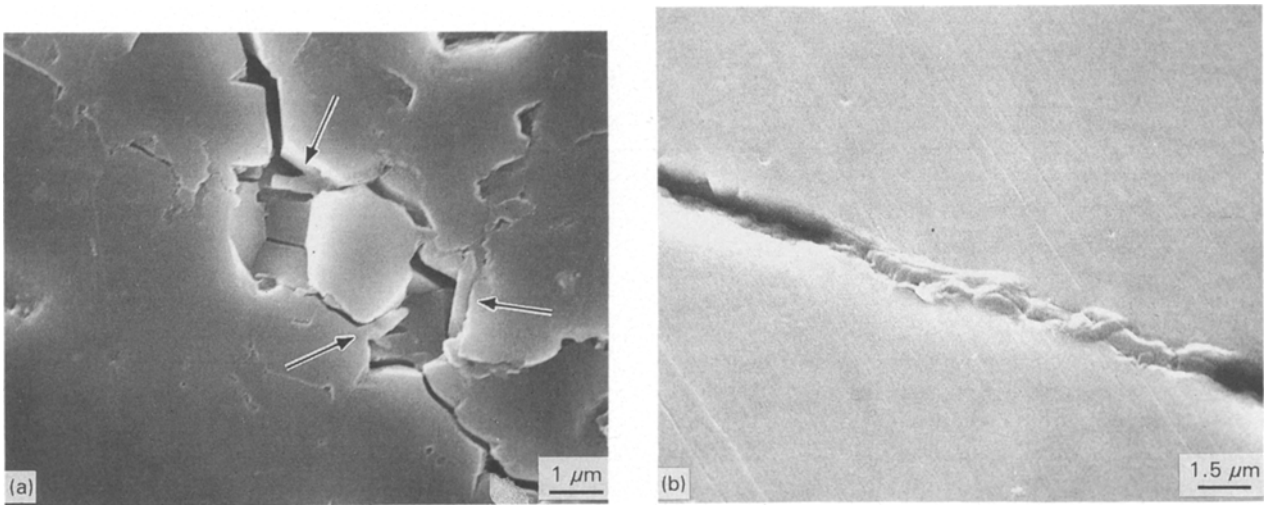

Figure 5 Indentation-produced crack paths revealing (a) whisker pull-out, crack bridging, and crack deflection phenomena, contributing to the toughness of Al_2O_3–10 vol % SiC_w and (b) no indication of either phenomenon, explaining the low toughness values of Al_2O_3–20 vol % SiC_w.

actions are believed to be partly responsible for the low toughness values observed in ZWTAs in this study and in a number of other studies [35–38].

A relatively high fracture toughness value was achieved in a partially shock-compacted (10 GPa) and 30 min pressureless-sintered sample (Table VI), considering that it had 4% porosity. Longer sintering times may improve such a sample's density and mechanical properties.

4. Conclusions

1. Shock-treatment of Al_2O_3 or Al_2O_3–ZrO_2 powders does not provide activated sintering. No significant difference is found in hot-pressed densities of alumina-based composites upon shock-treatment, compared to unshocked composites.

2. Sintered densities of alumina and ZTA decrease as the shock pressure and/or the amount of ZrO_2 is increased. This is attributed to shock-induced hard agglomerates in the former case and a higher frequency of ZrO_2 agglomerate formation in the latter.

3. Shock-compacted and sintered pellets of alumina and alumina-based composites attain higher fractional densities compared to their cold-pressed and sintered counterparts. This is attributed to the higher initial densities of shock-compacted samples compared to cold-pressed samples. The disadvantage of this method, however, is crack formation during any of the compaction, recovery, or sintering stages.

4. The fraction of t-ZrO_2 in the total (t + m) amount of ZrO_2 decreases as the amount of ZrO_2 increases in the alumina matrix in pressureless-sintered ZTA composites. This may be related to the lower relative densities attainable in shock-treated and unshocked ZTA composites with increasing ZrO_2 content, resulting in a reduced matrix constraint on ZrO_2 particles. Shock treatment has no significant effect on the amount of retained t-ZrO_2 in sintered or hot-pressed ZTA.

5. Chemical reaction of ZrO_2 and carbon supplied by SiC, carbon-rich furnace gases, or the graphite rams and dies used for hot pressing, leads to the formation of ZrC in ZWTA. Annealing of composites

containing ZrC in air causes total decomposition. Therefore, any high-temperature application of such composites in oxidizing environments would be disastrous.

Acknowledgements

The authors thank E. Cort, S. R. Skaggs, L. Trujillo, and K. Sickafus, Los Alamos National Laboratories, for their assistance with equipment, hot pressing, and TEM sample preparation. This work was supported by Los Alamos National Laboratories under Contract LANL 9XT 96721 R1, and is based on the thesis by M. Bengisu for the PhD degree in Materials Engineering, New Mexico Institute of Mining and Technology, Socorro, NM (1992).

References

1. J. WANG and R. STEVENS, *J. Mater. Sci.* **24** (1990) 3421.
2. F. F. LANGE and M. M. HIRLINGER, *J. Am. Ceram. Soc.* **67** (1984) 164.
3. R. DUCLOS, J. CRAMPON and B. CALES, *Ceram. Int.* **18** (1992) 57.
4. S. IIO, M. WATANABE, M. MATSUBARA and Y. MATSUO, *J. Am. Ceram. Soc.* **72** (1989) 1880.
5. P. F. BECHER, C. H. HSUEH, P. ANGELINI and T. N. TIEGS, *ibid.* **71** (1988) 1050.
6. E. A. HOLM and M. J. CIMA, *ibid.* **72** (1989) 303.
7. M. RUHLE, N. CLAUSSEN and A. H. HEUER, *ibid.* **69** (1986) 195.
8. T. N. TIEGS and P. F. BECHER, *Am. Ceram. Soc. Bull.* **66** (1987) 339.
9. V. K. SARIN and M. RUHLE, *Composites* **18** (1987) 129.
10. T. S. YEN and J. K. GUO, in "Advances in Ceramics", Vol. 24, "Science and Technology of Zirconia III", edited by S. Somiya, N. Yamamoto, and H. Yanagida (American Ceramic Society, Westerville, OH, 1988) pp. 573–82.
11. L. BJORK and A. G. HERMANSSON, *J. Am. Ceram. Soc.* **72** (1989) 1436.
12. H. W. LEE and M. D. SACKS, *Ceram. Eng. Sci. Proc.* **10** (1989) 720.
13. M. LEE and M. P. BOROM, *Adv. Ceram. Mater.* **3** (1988) 38.
14. M. BENGISU and O. T. INAL, *Ceram. Int.* **17** (1991) 187.
15. T. T. MEEK, R. D. BLAKE and J. J. PETROVIC, *Ceram. Eng. Sci. Proc.* **8** (1987) 861.
16. O. R. BERGMANN and J. BARRINGTON, *J. Am. Ceram. Soc.* **49** (1966) 502.
17. E. K. BEAUCHAMP, in "High Pressure Explosive Processing of Ceramics", edited by R. A. Graham and A. B. Sawaoka (Trans Tech, Switzerland, 1987) pp. 141–74.
18. R. R. GARCIA, "Dispersion of Oxide Powders in Organic Liquids", Ceramic Processing Research Laboratory Report No. 11, Jan. 1982, Department of Materials Science and Engineering, Massachusetts Institute of Technology, Cambridge, MA.
19. S. L. WANG, PhD thesis, New Mexico Institute of Mining and Technology, Socorro, NM (1986).
20. D. W. RICHERSON, "Modern Ceramic Engineering" (Marcel Dekker, New York, NY, 1982).
21. H. TORAYA, M. YOSHIMURA and S. SOMIYA, *J. Am. Ceram. Soc.* **67** (1984) C-119.
22. P. CHANTIKUL, G. R. ANSTIS, B. R. LAWN and D. B. MARSHALL, *J. Am. Ceram. Soc.* **64** (1981) 539.
23. M. V. SWAIN and N. CLAUSSEN, *J. Am. Ceram. Soc.* **66** (1983) C-27.
24. F. F. LANGE, *ibid.* **66** (1983) 396.
25. F. F. LANGE, B. I. DAVIS and I. A. AKSAY, *ibid.* **66** (1983) 407.
26. T. H. HARE, K. L. MORE, A. D. BATCHELOR and H. PALMOUR III, in "Materials Science Research", Vol. 16, "Sintering and Heterogeneous Catalysis", edited by G. C. Kuczynski, A. E. Miller and G. A. Sargent (Plenum Press, New York, NY, 1984) pp. 265–79.
27. S. WU, E. GILBART and R. J. BROOK, in "Advances in Ceramics", Vol. 10, "Structure and Properties of MgO and Al_2O_3 Ceramics", edited by W. D. Kingery (American Ceramic Society, Columbus, OH, 1984) pp. 574–82.
28. F. F. LANGE, in "Defect Properties of High Technology Nonmetallic Materials", edited by J. H. Crawford Jr, Y. Chen and W. A. Sibley (Elsevier Science, New York, NY, 1984) pp. 247–54.
29. M. BENGISU and O. T. INAL, *J. Am. Ceram. Soc.* **73** (1990) 346.
30. M. BACHAUS-RICOULT, *ibid.* **74** (1991) 1793.
31. S. T. BULJAN, A. E. PASTO and H. J. KIM, *Am. Ceram. Soc. Bull.* **68** (1989) 387.
32. N. CLAUSSEN, J. STEEB and R. F. PABST, *ibid.* **56** (1977) 559.
33. N. CLAUSSEN, *J. Am. Ceram. Soc.* **74** (1991) 1793.
34. M. BENGISU and O. T. INAL, *ibid.*, submitted.
35. N. CLAUSSEN, K. L. WEISSKOPF and M. RUHLE, *ibid.* **69** (1986) 288.
36. M. BOHMER and E. A. ALMOND, *Mater. Sci. Eng.* **A105/106** (1988) 105.
37. A. C. SOLOMAH, W. REICHERT, V. RONDINELLA, L. ESPOSITO and E. TOSCANO, *J. Am. Ceram. Soc.* **73** (1990) 740.
38. E. LUCCHINI and S. MASCHIO, *J. Mater. Sci. Lett.* **9** (1990) 417.

Received 10 March 1993
and accepted 28 February 1994